

# A central partition of molecular conformational space.

## I. Basic structures.

Jacques Gabarro-Arpa\*

LBPA, C.N.R.S. UMR 8532, Ecole Normale Supérieure de Cachan  
61, Avenue du Président Wilson, 94235 Cachan cedex, France

and

Ecole Normale Supérieure, C.N.R.S. FRE 2411  
Laboratoire Interdisciplinaire de Géométrie Appliquée  
45, rue d'Ulm, 75230 Paris cedex, France

### Abstract

On the basis of empirical evidence from molecular dynamics simulations, molecular conformational space can be described by means of a partition of central conical regions characterized by the dominance relations between cartesian coordinates. This work presents a geometric and combinatorial description of this structure.

---

\* Electronic Address: [jga@lbpa.ens-cachan.fr](mailto:jga@lbpa.ens-cachan.fr)

## Introduction

In previous works (Gabarro-Arpa and Revilla, 2000, Laboulais *et al.*, 2002) it was put forward the idea that the three-dimensional structure of proteins could be encoded into binary sequences. For a molecule with  $N$  atoms in a given conformation the procedure employed consisted in

- defining a procedure for enumerating the atoms, which gives an order relation,
- forming the set of all ordered sets of four atoms (4-tuples), with size  $P = \binom{N}{4}$ ,
- as in the mesoscopic models of macromolecules atoms are represented by pointlike structures, a 4-tuple determines a 3-simplex<sup>†</sup>, since the atoms in the 4-tuples are ordered a given 3-simplex can be left or right handed. Depending on the simplex handedness each 4-tuple is given a sign  $+/-$ ,
- the set of 4-tuples can also be ordered to become a sequence, from it and the signs associated to each 4-tuple a sign vector  $\{+, -\}^P$  can be constructed: the **chirotope**<sup>‡</sup>, which is the desired binary sequence.

The chirotope defines an equivalence relation between conformations: two conformations belong to the same equivalence class if they have the same chirotope. This generates a geometrical structure in conformational space: a partition  $\mathcal{X}$  into a set of regions (cells) whose points (3D-conformations) have all the same chirotope.

The connected components of such equivalence classes are locally compatible with a central conical geometry: multiplying the  $3 \times N$  cartesian coordinates of a given conformation by an arbitrary positive factor does not change the chirotope, since under this transformation the handedness of a scaled 3-simplex remains unchanged. Thus, in conformational space the set of points lying on a half-line starting at the origin all belong to the same equivalence class. The term **central** means that the vertices of the cones are at the origin. In the following, if we talk about a **partition** without further qualifications, we mean a central partition.

This simple result suggests that conformational space can be partitioned into a discrete set of conical cells, the structure of this partition is encoded by the **graph of regions**  $\mathcal{T}(\mathcal{X})$ , which has as vertices the set of cells of  $\mathcal{X}$  and as edges the pairs of cells that are adjacent.

Since the graph is connected, there is a graphical distance between cells as the length of the shortest path between the two representative vertices in the graph. The same distance between two equivalence classes can be defined as a Hamming distance: the number of different signs between the chirotopes of the two conformations. The latter definition was first employed in (Gabarro-Arpa and Revilla, 2000), where no geometrical interpretation in terms of space partition was attempted.

In the two works cited above the Hamming distance was used to analyze clusters of conformations in molecular dynamics trajectories with measurably good results, in these studies when compared with the classical r.m.s. deviation measure (Kabsch, 1978) it was seen to perform better and to be more robust (Laboulais *et al.*, 2002). This good performance can be qualitatively explained if the mesh that results from projecting the graph of regions onto the hypersurface where the system evolves, is sufficiently fine grained to give an accurate measure, at least in the range explored by molecular dynamics simulations.

Thus it seems not unreasonable to give a description of conformational space based on a central partition of conical cells. However, working out the set of cells derived from the chirotope turns

---

<sup>†</sup> a three-dimensional (3D) polytope with four vertices.

<sup>‡</sup> in this work bold faced words refer to topics that are more fully developed in (Rosen, 2000) and references therein.

out not to be practical, so in this paper we present a partition derived from a central hyperplane arrangement, where a set of non-coplanar hyperplanes passing through the origin divide the space in a number of conical regions<sup>§</sup>.

### A central hyperplane arrangement

In what follows  $\mathbb{R}^N$  is a real affine space of  $N$  dimensions, and  $\{\mathbf{e}_i\}$ , with  $1 < i < N$ , are its unit vectors. We define the following set of vectors

$$\mathbf{N} = \{\mathbf{n}_{ij} = \mathbf{e}_i - \mathbf{e}_j, 1 \leq i < j \leq N\} \quad (1)$$

Notice that if  $\mathbf{u} = (1, \dots, 1)$  and  $\mathbf{n}_{ij} \in \mathbf{N}$  then  $\mathbf{u} \cdot \mathbf{n}_{ij} = 0$ .

Associated with this set there is a set of central non-coplanar hyperplanes

$$\mathcal{H}_{ij}(p) = \{p \in \mathbb{R}^N : \mathbf{n}_{ij} \cdot p = 0\} \quad (2)$$

each hyperplane divides  $\mathbb{R}^N$  into the positive and negative hemispaces

$$\mathcal{H}_{ij}^+(p) = \{p \in \mathbb{R}^N : \mathbf{n}_{ij} \cdot p > 0\}, \quad \mathcal{H}_{ij}^-(p) = \{p \in \mathbb{R}^N : \mathbf{n}_{ij} \cdot p < 0\}$$

so the hyperplane arrangement determines a partition  $\mathcal{P}$  of  $\mathbb{R}^N$  into a set of convex regions (cells), where each cell  $\mathcal{C} \in \mathcal{P}$  can be characterized by an antisymmetric  $N \times N$  sign matrix  $\mathcal{V}$ , such that if  $p \in \mathcal{C}$  then

$$\mathcal{V}_{ii} = 0, \quad \mathcal{V}_{ij} = \begin{cases} + & p \in \mathcal{H}_{ij}^+ \\ 0 & p \in \mathcal{H}_{ij} \\ - & p \in \mathcal{H}_{ij}^- \end{cases}, \quad \mathcal{V}_{ji} = \begin{cases} - & \\ 0 & \\ + & \end{cases} \quad \forall i < j \quad (3)$$

The geometrical meaning of the sign matrix can be easily deduced from the following example: let  $p^a, p^b \in \mathbb{R}^N$  be two points with coordinates

$$p^a = (1, 2, 3, 4, 5, \dots, N) \\ p^b = (1, 2, 4, 3, 5, \dots, N)$$

obviously  $\mathcal{V}^a = \{\mathcal{V}_{ij}^a = +, \forall i < j\}$  is the sign matrix of  $p^a$ . Now  $p^b$  has the same matrix except that  $\mathcal{V}_{34}^b = -$ . Thus, for any point  $p$  the sign matrix encodes the pairwise dominance relations between its coordinates

$$\mathcal{V}_{ij} = \begin{cases} + & p_i < p_j \\ 0 & p_i = p_j \\ - & p_i > p_j \end{cases} \quad \forall i < j$$

In the above example notice also that  $\mathbf{n}_{34} = p^b - p^a$  (4).

Let  $\pi(N)$  be the set of points in  $\mathbb{R}^N$  whose coordinates are the permutations of the sequence  $\{1, 2, 3, 4, 5, \dots, N\}$ , no two points in this set have the same  $\mathcal{V}$  matrix, and since it encodes the complete set of dominance relations between coordinates, there is a one to one correspondence between  $\pi(N)$  and  $\mathcal{P}$ , making a total of  $N!$  cells in  $\mathcal{P}$ .

### The graph of regions of the arrangement

In order to study the graph of regions  $\mathcal{T}(\mathcal{P})$ , it is important to notice that  $\mathcal{V}$  is the incidence matrix of an **acyclic tournament** (Moon, 1968).

Tournaments are directed graphs such that between any two nodes there is always an arc (see example in fig. 1), if  $v_i$  and  $v_j$  are two nodes,  $\mathcal{V}_{ij} = +$  if the arc goes from  $i$  to  $j$ , we say that  $v_i$

---

<sup>§</sup> In what follows the term **cone** means a region of space determined by a set of vectors in  $\mathbb{R}^N$  such that for any finite subset of vectors it also contains all their linear combinations with positive coefficients.

**dominates**  $v_j$ ; otherwise  $\mathcal{V}_{ij} = -$  and  $v_i$  is dominated by  $v_j$ .

The **acyclic**<sup>¶</sup> qualifier is because there are no directed cycles in the graph (as can be seen in fig. 1). This is a particularity of the tournaments that characterize the cells of  $\mathcal{P}$ : for any permutation there are always two nodes called the **source** and the **sink** respectively, the former dominates all other nodes and the latter is dominated by every node in the graph (nodes 3 and 2 in fig. 1, respectively). Moreover it is a **centrally symmetric hierarchical** structure:

- the graph that results from reversing all the arcs is also acyclic,
- deleting a node always gives a subtournament.

This tells us that each  $N$ -dimensional cell in  $\mathcal{P}$  has exactly  $N - 1$  neighbours, since there are exactly  $N - 1$  arcs in a tournament that can be reversed without creating a directed cycle. These are the arcs joining nodes whose score differs by 1 (see the legend of fig. 1).

$\mathcal{T}(\mathcal{P})$  can be obtained by joining with a line segment the points in  $\pi(N)$  that are in adjacent cells, the result is the 1-**skeleton** of a convex polytope: the  $N$ -**permutohedron** or  $\Pi_{N-1}$  (Schoute, 1911).

The study of the faces of  $\Pi_{N-1}$  is an essential part in our study of  $\mathcal{P}$ , since it allows conformations and groups of conformations to be accurately located within  $\Pi_{N-1}$ .

### The faces of $\Pi_{N-1}$

Central to this construction is the duality between the faces of  $\Pi_{N-1}$  and the cells of  $\mathcal{P}$ :  $k$ -faces and cells of dimension  $N - k$  lie in orthogonal linear subspaces. The sign matrix of lower dimensional cells has zeros in the entries corresponding to hyperplanes that contain the cell, as defined in (3), this matrix can be represented by incomplete tournaments: these are digraphs where the arcs corresponding to the zero entries have been deleted (see fig. 2).

Incomplete tournaments can be seen as patterns: we say that a given tournament matches a *pattern* if both graphs have the same **order** and if the pattern is a subgraph of the tournament.

The simplest non-trivial faces in the hierarchy are the 1-faces: edges that join adjacent vertices (0-faces). As we have seen, adjacent vertices differ in that they exchange the value of two coordinates, say  $\mathbf{i}$  and  $\mathbf{j}$ , and the edge is parallel to the vector  $\mathbf{n}_{ij}$  (4), which is perpendicular to the hyperplane  $\mathcal{H}_{ij}$ . This hyperplane contains the  $(N - 1)$ -dimensional boundary cell that separates the  $N$ -dimensional cells of the vertices, accordingly its sign matrix has  $\mathcal{V}_{ij} = \mathcal{V}_{ji} = 0$ .

The pattern of fig. 2a, where the arc between  $v_2$  and  $v_6$  is missing, matches exactly two tournaments that represent the vertices of the edge segment, also the complement graphs<sup>||</sup> of these vertices is a set of lower order tournaments that encode the vertices of a lower dimensional permutohedron. In our case we have two order 2 tournaments (one can be seen in fig. 3a), that represent the permutations of the sequence  $\{56\}$ : the associated permutohedron is a line segment.

On the other extreme lets look at the  $(N - 2)$ -faces. Notice that for the hyperplane arrangement described above if we construct the vector

$$\mathbf{u}^\alpha = \{\mathbf{u}_\alpha^\alpha = 1 - N, \mathbf{u}_i^\alpha = 1, i \neq \alpha, 1 \leq i \leq N\} \quad (5)$$

where  $1 \leq \alpha \leq N$ ; the set of vectors

$$\mathbf{N}^\alpha = \{\mathbf{n}_{ij} \in \mathbf{N} : 1 \leq \mathbf{i} < \mathbf{j} \leq N, \mathbf{i} \neq \alpha, \mathbf{j} \neq \alpha\} \quad (6)$$

and the subset of hyperplanes

---

<sup>¶</sup> All along this work tournaments are implicitly assumed to be acyclic.

<sup>||</sup> Given a tournament  $T$  and a pattern  $P$  the *complement graph* is a graph with the edges that are in  $T$  but not in  $P$  and the vertices that are in those edges (see fig. 3).

$$\mathcal{H}^\alpha = \{\mathcal{H}_{ij}(p) : \mathbf{n}_{ij} \cdot p = 0, \mathbf{n}_{ij} \in \mathbf{N}^\alpha, p \in \mathbb{R}^N\}$$

we have  $\mathbf{u}^\alpha \cdot \mathbf{n}_{ij} = 0$  for all  $\mathbf{n}_{ij} \in \mathbf{N}^\alpha$ . This means that the vectors in  $\mathbf{N}^\alpha$  are all in the  $(N-1)$ -hyperplane  $\mathbf{u}^\alpha \cdot p = 0$ , consequently

- the hyperplanes in  $\mathcal{H}^\alpha$  all have a common intersection: a 2-hyperplane parallel to  $\mathbf{u}^\alpha$ ,
- the set of vertices in the  $N$ -cells adjacent to this 2-cell all lie in a  $(N-2)$ -hyperplane: they are the vertices of a  $(N-2)$ -face,
- as can be deduced from (5) and (6), the only arcs present in the pattern of this face are those that connect node  $\alpha$  to the other nodes,
- node  $\alpha$  is either a source or a sink.

For  $N = 6$  we have the example pattern of fig. 2b, fig. 3b shows the complement graph which is a  $N = 5$  tournament, the set of all complement graphs encodes the permutations of the set  $\{12345\}$ , and hence the corresponding face is a  $\Pi_4$  polytope. This tells us that a total of  $2N$  faces of  $\Pi_{N-1}$  are  $\Pi_{N-2}$  polytopes.

Before proceeding further we must introduce the basic notion of **product polytope**. If  $P$  is a polytope in  $\mathbb{R}^p$  and  $Q$  a polytope in  $\mathbb{R}^q$  then the product polytope  $P \times Q$  is defined as the set of all vertices  $(x, y) \in \mathbb{R}^{p+q}$  such that  $x \in \mathbb{R}^p$  is a vertex of  $P$  and  $y \in \mathbb{R}^q$  is a vertex of  $Q$ . Examples of product polytopes are: the square which is the product of two segments (two polytopes of dimension 1). The cube which is the product of a square by a segment, more generally the prisms, which are the product of a polygon (or polytope) by a segment.

The example pattern from fig. 2c encodes a product polytope: the set of compatible subtournaments formed by vertices  $v_1, v_3, v_4$  and  $v_5$ , encode a  $\Pi_3$ , and are independent from the subtournament formed by  $v_2$  and  $v_6$  which encodes a segment (or  $\Pi_1$ ). Thus there are  $N \times (N-1)$   $(N-2)$ -dimensional faces which are prisms joining two  $\Pi_{N-3}$  from adjacent  $\Pi_{N-2}$  faces.

It can be easily seen that all the faces from this polytope are either permutohedrons or products of permutohedrons, for instance the polytope encoded by the pattern of fig. 2d is a  $\Pi_1 \times \Pi_1 \times \Pi_1$ , that is: a cube.

Notice that for the product of permutohedrons the complement graphs (see figs. 3c and 3d) are not connected.

### The face lattice of $\Pi_{N-1}$

The differences among incomplete tournaments, when we disregard the identity of the nodes, arise from the topology of the graph: number of edges and nodes, and the connectivity. We can define an operation on patterns that consists in renumbering the nodes so that the score never decreases upon increasing the node number. Renumbered patterns are stripped from the complications that arise from permuting equivalent nodes, a classification of these objects based on topological differences, is far more simple while keeping their essential characteristics, it results in a comprehensive synthetic view of the face arrangement. Introducing the permutations between equivalent nodes is an unnecessary complication that can always be worked out in a later stage.

The set of equivalence classes obtained upon renumbering is isomorph to the set  $\mathcal{L}$  of partitions of the sequence  $\{1, 2, 3, \dots, N\}$  into subsets of consecutive integers. The correspondence is established as follows

- for each incomplete tournament form a sequence with the partial scores arranged in ascending order
- divide this sequence into subsets of identical partial scores

- replace each element in a subsequence of identical scores by the the corresponding node number in the renumbered sequence.

For instance from the graph of fig. 2b we form the sequence 111116, whose corresponding partition is (12345)6. Likewise, for figs. 2a, 2c and 2d the sequences 123455, 111155 and 113355, give the partitions 1234(56), (1234)(56) and (12)(34)(56) respectively. These partitions represent classes of polytopes that are combinatorially equivalent, there are  $N!/(n_1! \times n_2! \times \dots)$  elements in each class,  $n_i$  being the number of elements in each subset. Notice that (56), for instance, represents the set of permutations of the sequence {56}

There is a partial order in the set of partitions, it is based on containment: we say that a partition set  $x$  is contained in  $y$  ( $x \subset y$ ), if each subset in  $x$  is either identical to a subset of  $y$  or it is a subset of some subset in  $y$ . Thus for the above example:  $1234(56) \subset (12)(34)(56) \subset (1234)(56)$ , also  $(1234)56 \subset (1234)(56)$  and  $(1234)56 \subset (12345)6$ , but  $(1234)(56) \not\subset (12345)6$ .

It can be shown that the partially ordered set (**poset**)  $\mathcal{L}$  thus defined is a **lattice**, that is: for all pairs  $x, y \in \mathcal{L}$  there is a least upper bound and a greatest lower bound.

The lattice poset  $\mathcal{L}$  for  $N = 6$  is represented in fig. 4, each element represents a class of faces of  $\Pi_5$ , they are arranged in five rows, the faces in a row have the same dimension which increases from 0 in the bottom row to 5 at the top. There are  $\binom{N-1}{d}$  ( $0 \leq d \leq N$ ), elements in each row.

It should be noticed from fig. 4 the hierarchical structure of  $\mathcal{L}$ : each interval\*\* between a given element in the lattice and the minimal element 123456 is also a lattice. Which is an expected result: the face lattice of any face is in the face lattice.

## A partition of conformational space

The partition discussed in the previous sections is based on the dominance relations among the coordinates of points in an  $N$ -dimensional space, in conformational space the coordinates of each point are the coordinates of a set of  $N$  points in 3D cartesian space, as 3D cartesian coordinates are independent of each other it would make little sense to translate automatically the partition described above to a  $3 \times N$ -dimensional space, instead we propose the partition  $\mathcal{P}^3$  which is the union of three separate partitions:  $\mathcal{P}_x$ ,  $\mathcal{P}_y$  and  $\mathcal{P}_z$ , that encode the dominance relations among the  $x$ ,  $y$  and  $z$  coordinates of the set of points respectively.  $\mathcal{P}_x$ , for instance, is generated by the set of hyperplanes

$$\mathcal{H}_{ij}^x(p) = \{p \in \mathbb{R}^{3 \times N} : \mathbf{n}_{ij}^x \cdot p = 0\}$$

with a set of normal vectors defined as

$$\mathbf{N}^x = \{\mathbf{n}_{ij}^x = \mathbf{e}_i^x - \mathbf{e}_j^x, 1 \leq i < j \leq N\}$$

where the  $\mathbf{e}^x$  are the unit vectors in  $\mathbb{R}^{3 \times N}$  of the  $x$  coordinates of the 3D points.

$\mathbb{R}^{3 \times N}$  can be seen as a product space  $\mathbb{R}^N \times \mathbb{R}^N \times \mathbb{R}^N$ , with each factor harboring the  $x$ ,  $y$  and  $z$  coordinates of the set of points. Thus, as the dual polytope of  $\mathcal{P}_x$ , for instance, is  $\Pi_{N-1}$ , obviously the dual of  $\mathcal{P}^3$  will be  $\Pi_{N-1}^3 = \Pi_{N-1} \times \Pi_{N-1} \times \Pi_{N-1}$ , its face poset can be worked out from the observation that  $\Pi_{N-1}^3$  is a  $(3N-3)$ -face of  $\Pi_{3N-1}$ . See for example the symmetric class of faces (12)(34)(56) in fig. 4, the poset of  $\Pi_1^3$  is the interval 123456 – (12)(34)(56).

Now the question that arises is: how well do 3D  $N$  point sets arising from the vertices of  $\Pi_{N-1}^3$  relate to the actual conformations of macromolecules ?

An alternative representation of permutations is as 0/1 **matrices**, these are objects whose only entries are 0s and 1s with the entry 1 occuring exactly once in each column. As an example to the permutation encoded by the tournament of fig. 1 it corresponds the 0/1 matrix

---

\*\* An **interval** is a subposet which contains all elements  $z$  such that  $x \subseteq z \subseteq y$ .

$$\begin{pmatrix} 0 & 1 & 0 & 0 & 0 & 0 \\ 0 & 0 & 0 & 0 & 0 & 1 \\ 0 & 0 & 0 & 0 & 1 & 0 \\ 1 & 0 & 0 & 0 & 0 & 0 \\ 0 & 0 & 0 & 1 & 0 & 0 \\ 0 & 0 & 1 & 0 & 0 & 0 \end{pmatrix}$$

likewise the coordinates of a vertex in  $\Pi_{N-1}^3$  can be encoded by a three-dimensional 0/1 matrix, which can be regarded as a cubic lattice with only one site occupied per row in every dimension. Analogously, we can imagine in 3D cartesian space an  $N$ -point set embedded in a cubic lattice with cell spacing of 1 spanning a rectangle between 1 and  $N$  in every dimension with the points located at the intersections such that there is only one point in every row in any dimension.

We can compare in fig. 5 the 3D stereoviews of the HIV-1 integrase catalytic core  $C_\alpha$  skeleton (fig. 5a)<sup>††</sup>, with the 3D representation, fig. 5b, of the corresponding  $\Pi_{162}^3$  vertex within the  $\mathcal{P}^3$  cell. Although fig. 5b appears to be somewhat deformed with respect to fig. 5a, all the characteristic folding patterns:  $\alpha$ -helices,  $\beta$ -sheets, turns ... appear to be conserved.

This means that a lot of the 3D structure is encoded by the set of dominance relations among the cartesian coordinates of individual atoms.

## Conclusion

Most of the time conformational space is referenced as an abstract paradigm too complex to be understood. The aim of this work is to show that the geometry of conformational space is not beyond the reach of mathematical intuition: with the help of adequate mathematical structures its sheer complexity can be brought to tractable dimensions, and it can be done with existing and well understood mathematical tools.

The model developed here offers a number of interesting possibilities

- the structural diversity of a macromolecule can be explored by means of combinatorial patterns
- the classification of conformations can give a catalog of structures
- graphical paths can be used to determine and explore the paths between any two conformations
- its hierarchical structure makes it modular

There are shortcomings too: the present model shows a loss of precision in the 3D-structures obtained; but this should not be a major problem:

- precision can be recovered with the help of *ad hoc* methods. Optimization of structures within a cell should not be difficult
- there is no limit to the refinements that can be introduced into this basic model, in particular it should not be hard to build smaller cells, or to cut the existing ones into finer slices.

The possibilities offered by the model will be the subject of the forthcoming works.

---

<sup>††</sup>residues 50-212 of the integrase (Maignan *et al.*, 1998).

## References

- Gabarro-Arpa, J. and Revilla, R. (2000) *Comput. and Chem.* **24**, 693-698.
- Kabsch, W. (1978) *Acta Cryst.* **A34** 827-828.
- Laboulais, C., Ouali, M., Le Bret, M. and Gabarro-Arpa, J. (2002) *Proteins: Structure, Function, and Genetics* **47** 169-179.
- Maignan, S., Guilloteau, J. P., Zhou-Liu, Q., Clément-Mella, C., Mikol, V. (1998) *J. Mol. Biol.* **282** 359-368.
- Moon, J. W. (1968) *Topics on Tournaments* , Holt, Rinehart and Winston, New York.
- Rosen, K. editor in chief (2000) *Handbook of Discrete and Combinatorial Mathematics* CRC Press, New York.
- Schoute, P. H. (1911) *Verhandelingen der Koninklijke Akademie van Wetenschappen te Amsterdam*, Deel **11**, No. 3, Johannes Muller, Amsterdam, 1-87.



# Legends of Figures

## Figure 1

$N = 6$  tournament corresponding to the sign matrix

$$\mathcal{V} = \begin{pmatrix} 0 & - & + & + & - & - \\ + & 0 & + & + & + & + \\ - & - & 0 & - & - & - \\ - & - & + & 0 & - & - \\ + & - & + & + & 0 & - \\ + & - & + & + & + & 0 \end{pmatrix}$$

The **score** of a node is the number of nodes it dominates plus 1 (in order to establish a correspondence with permutations). It is annotated above each node in the figure.

## Figure 2

Example incomplete tournaments for  $N = 6$  matching the tournament of fig. 1. Their respective sign matrices are

$$\mathcal{V}^a = \begin{pmatrix} 0 & - & + & + & - & - \\ + & 0 & + & + & + & 0 \\ - & - & 0 & - & - & - \\ - & - & + & 0 & - & - \\ + & - & + & + & 0 & - \\ + & 0 & + & + & + & 0 \end{pmatrix} \quad \mathcal{V}^b = \begin{pmatrix} 0 & - & 0 & 0 & 0 & 0 \\ + & 0 & + & + & + & + \\ 0 & - & 0 & 0 & 0 & 0 \\ 0 & - & 0 & 0 & 0 & 0 \\ 0 & - & 0 & 0 & 0 & 0 \\ 0 & - & 0 & 0 & 0 & 0 \end{pmatrix}$$

$$\mathcal{V}^c = \begin{pmatrix} 0 & - & + & + & - & - \\ + & 0 & + & + & + & 0 \\ - & - & 0 & 0 & - & - \\ - & - & 0 & 0 & 0 & - \\ + & - & + & 0 & 0 & - \\ + & 0 & + & + & + & 0 \end{pmatrix} \quad \mathcal{V}^d = \begin{pmatrix} 0 & - & + & + & 0 & - \\ + & 0 & + & + & + & 0 \\ - & - & 0 & 0 & - & - \\ - & - & 0 & 0 & - & - \\ 0 & - & + & + & 0 & - \\ + & 0 & + & + & + & 0 \end{pmatrix}$$

## Figure 3

Complement graphs of the tournament in fig. 1 with respect to the patterns in fig. 2.

## Figure 4

Poset  $\mathcal{L}$  of the partitions of the sequence (123456) into subsets of consecutive integers. The bold letters above some partitions refer to the incomplete tournaments in fig. 2.

## Figure 5

- a) Stereo drawing of the HIV-1 integrase catalytic core  $C_\alpha$  skeleton (residues 50-212 of the integrase, Maignan *et al.*, 1998).
- b) Stereo drawing of the related vertex in  $\Pi_{162}^3$ .

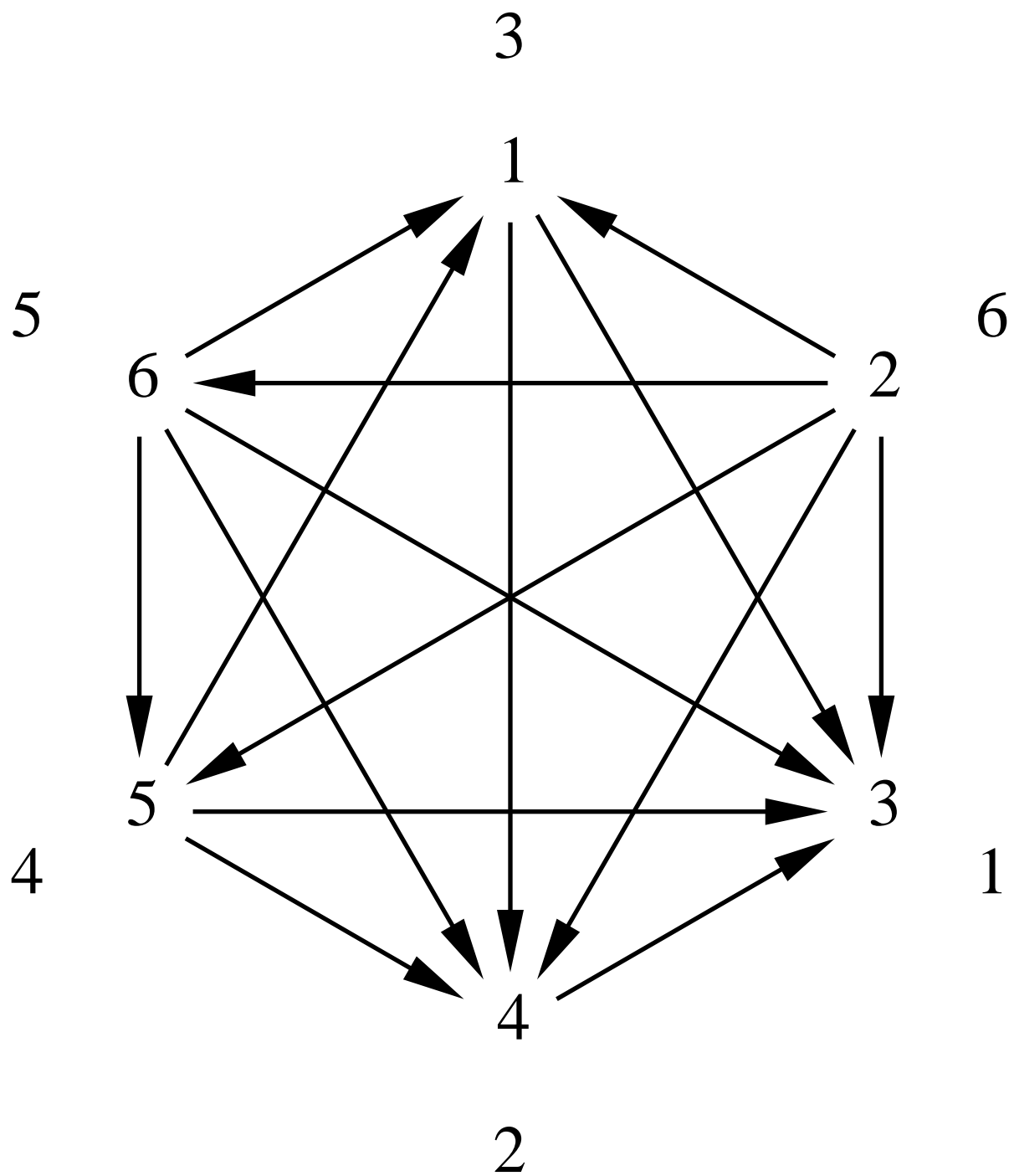


Figure 1

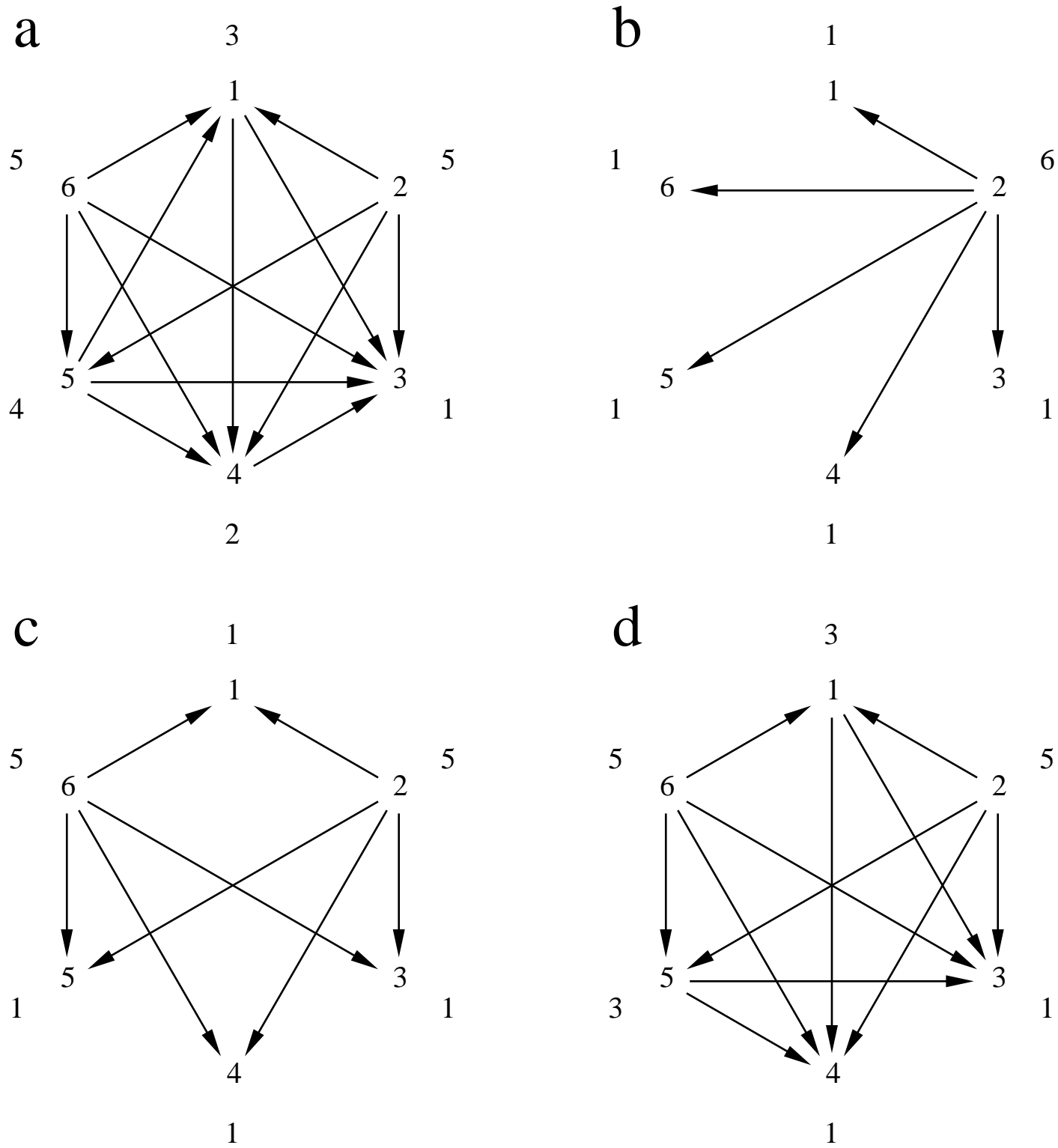
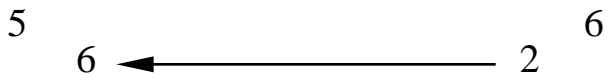
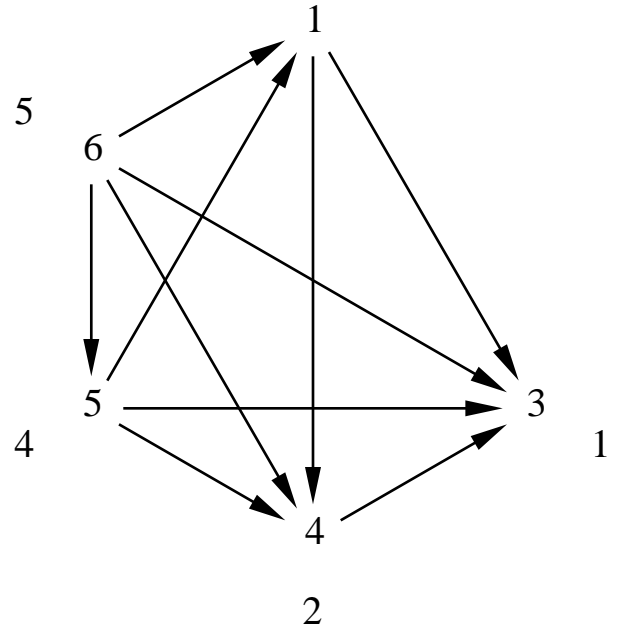


Figure 2

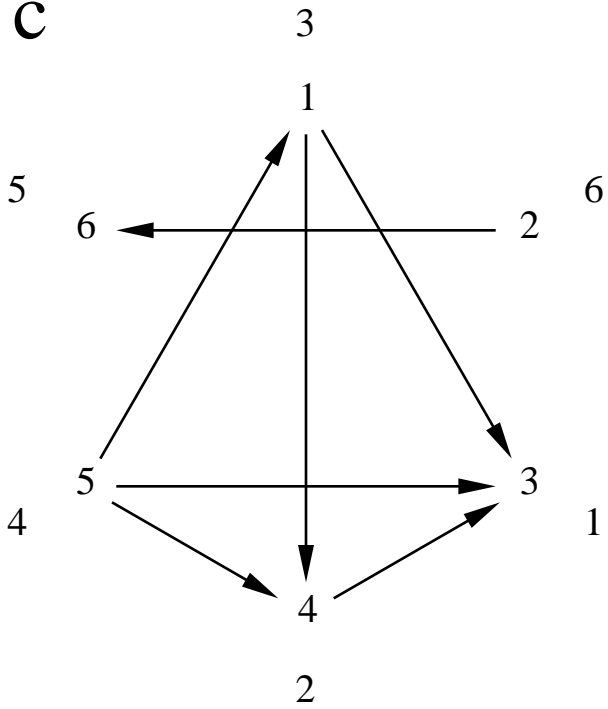
a



b



c



d

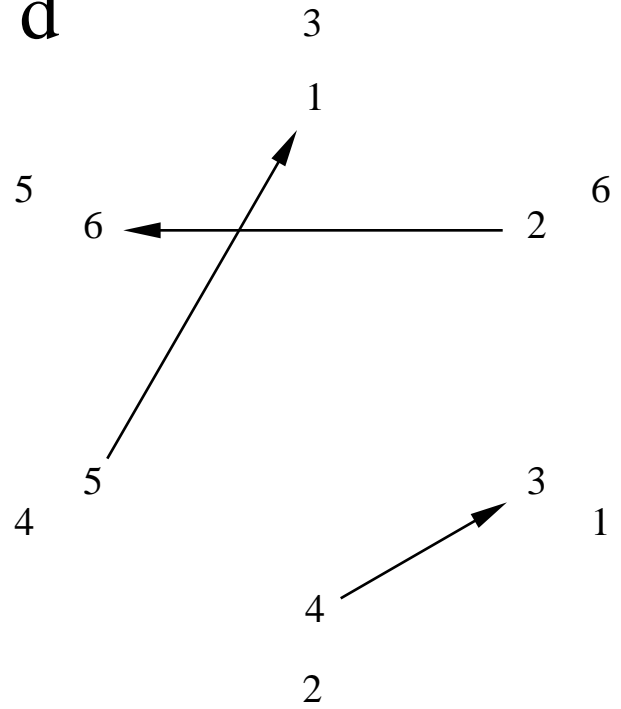


Figure 3

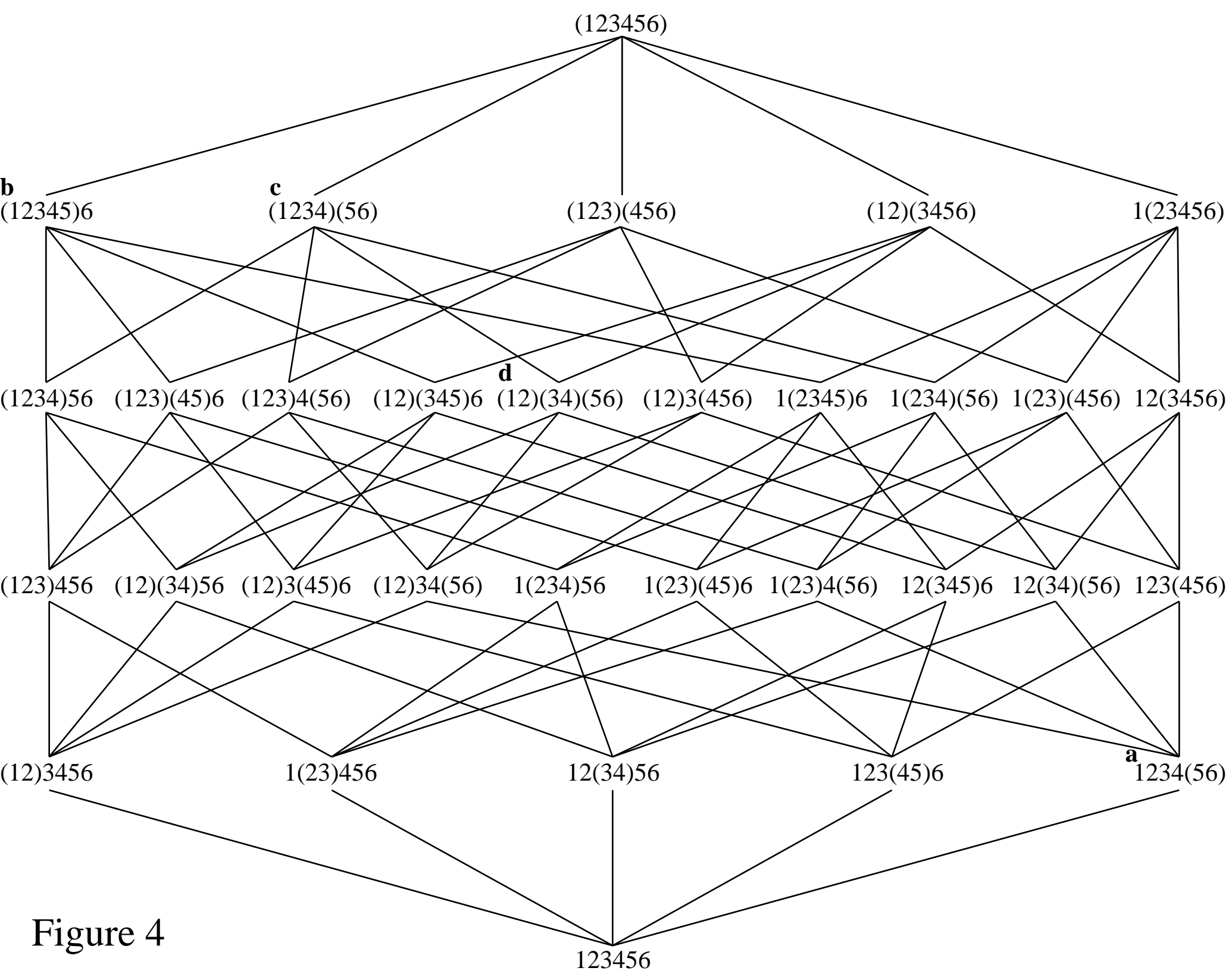
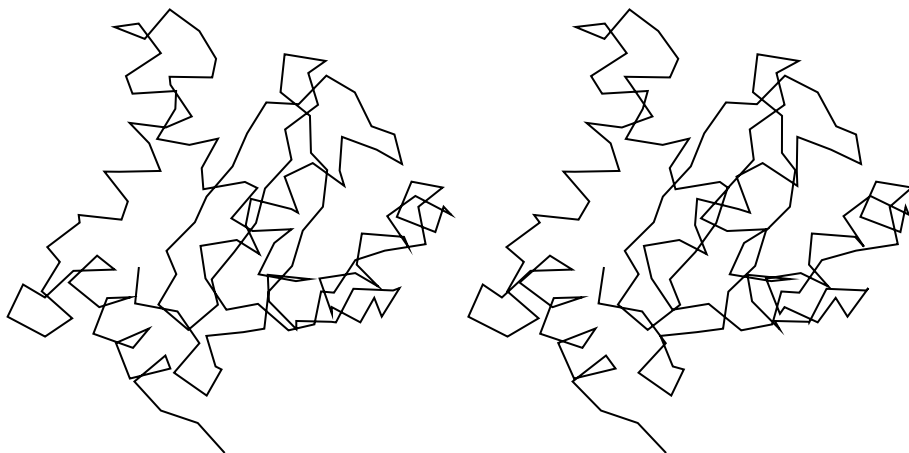


Figure 4

a



b

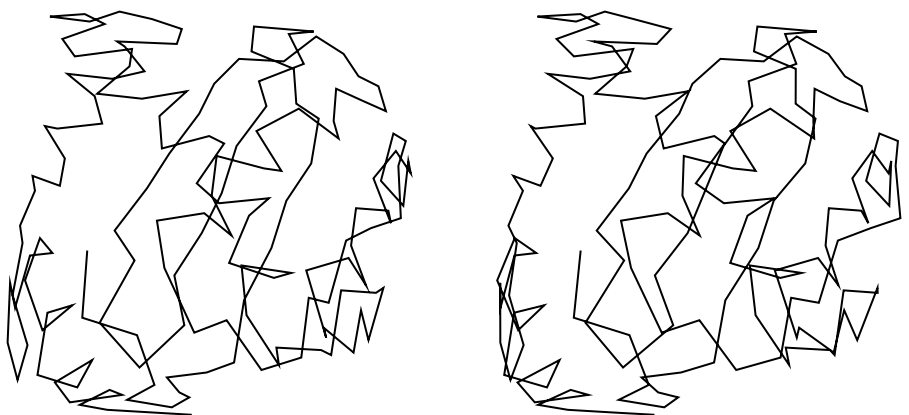


Figure 5